

Timelike vs spacelike DVCS from JLab, Compass to ultraperipheral collisions and AFTER@LHC *

H. Moutarde ¹, B. Pire ², F. Sabatié ¹, L. Szymanowski ³ and J. Wagner ³

1. Irfu-SPhN, CEA, Saclay, France

2. CPhT, École polytechnique, CNRS, 91128 Palaiseau, France

3. National Centre for Nuclear Research (NCBJ), Warsaw, Poland

June 30, 2021

Abstract

Timelike and spacelike virtual Compton scattering in the generalized Bjorken scaling regime are complementary tools to access generalized parton distributions. We stress that the gluonic contributions are by no means negligible, even in the medium energy range which will be studied intensely at JLab12 and in the COMPASS-II experiment at CERN. Ultraperipheral collisions with proton or ion beams may also be used at RHIC and at collider or fixed target experiments at LHC.

1 Introduction

In the collinear factorization framework the scattering amplitudes for exclusive processes such as deeply virtual Compton scattering (DVCS) [1]

$$\gamma^*(q_{in})N(P) \rightarrow \gamma(q_{out})N'(P' = P + \Delta), \quad q_{in}^2 = -Q^2 < 0, \quad q_{out}^2 = 0, \quad (1)$$

and its crossed reaction, timelike Compton scattering (TCS) [2]

$$\gamma(q_{in})N(P) \rightarrow \gamma^*(q_{out})N'(P' = P + \Delta), \quad q_{in}^2 = 0, \quad q_{out}^2 = Q^2 > 0, \quad (2)$$

have been shown to factorize in specific kinematical regions, provided a large scale controls the separation of short distance dominated partonic subprocesses and long distance hadronic matrix elements, the generalized quark and gluon distributions (GPDs) [3] which encode much information on the partonic content

*Presented at the Low x workshop, May 30 - June 4 2013, Rehovot and Eilat, Israel

of nucleons. After factorization, the DVCS (and similarly TCS) amplitudes are written in terms of Compton form factors (CFF) \mathcal{H} , \mathcal{E} and $\tilde{\mathcal{H}}$, $\tilde{\mathcal{E}}$, as :

$$\begin{aligned} \mathcal{A}^{\mu\nu}(\xi, t) = & -e^2 \frac{1}{(P+P')^+} \bar{u}(P') \left[g_T^{\mu\nu} \left(\mathcal{H}(\xi, t) \gamma^+ + \mathcal{E}(\xi, t) \frac{i\sigma^{+\rho} \Delta_\rho}{2M} \right) \right. \\ & \left. + i\epsilon_T^{\mu\nu} \left(\tilde{\mathcal{H}}(\xi, t) \gamma^+ \gamma_5 + \tilde{\mathcal{E}}(\xi, t) \frac{\Delta^+ \gamma_5}{2M} \right) \right] u(P), \end{aligned} \quad (3)$$

with the CFFs defined as

$$\begin{aligned} \mathcal{H}(\xi, t) &= + \int_{-1}^1 dx \left(\sum_q T^q(x, \xi) H^q(x, \xi, t) + T^g(x, \xi) H^g(x, \xi, t) \right), \\ \tilde{\mathcal{H}}(\xi, t) &= - \int_{-1}^1 dx \left(\sum_q \tilde{T}^q(x, \xi) \tilde{H}^q(x, \xi, t) + \tilde{T}^g(x, \xi) \tilde{H}^g(x, \xi, t) \right). \end{aligned} \quad (4)$$

We report in Sect. 2 on a recent NLO analysis [4, 5] of DVCS and TCS amplitudes., and make a few remarks on the study of TCS in ultraperipheral collisions at hadron colliders (Sect. 3) and at fixed target experiments at LHC (Sect. 4).

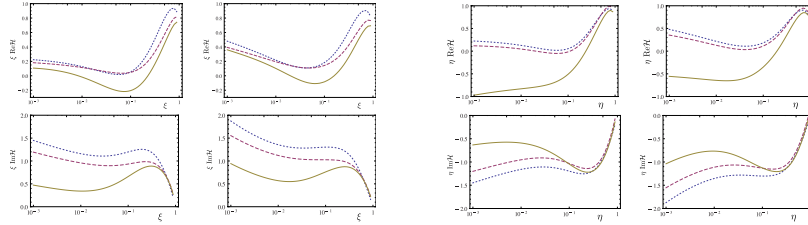


Figure 1: The real (upper panels) and imaginary (lower pannels) parts of the *spacelike* $\mathcal{H}(\xi)$ (1st and 2nd columns) and *timelike* $\mathcal{H}(\eta)$ (3rd and 4th columns) Compton Form Factor multiplied by ξ (or η), in the double distribution model based on GK (1st and 3rd columns) and MSTW08 (2nd and 4th columns) parametrizations, for $\mu_F^2 = Q^2 = 4\text{GeV}^2$ and $t = -0.1\text{GeV}^2$. In all plots, the LO result is shown as the dotted line, the full NLO result by the solid line and the NLO result without the gluonic contribution as the dashed line.

2 On the importance of gluonic contributions

2.1 Gluonic effects to Compton form factors

TCS and DVCS amplitudes are identical (up to a complex conjugation) at lowest order in α_S but differ at next to leading order, in particular because of the quite different analytic structure of the scattering amplitudes of these reactions. Indeed, the production of a timelike photon enables the production

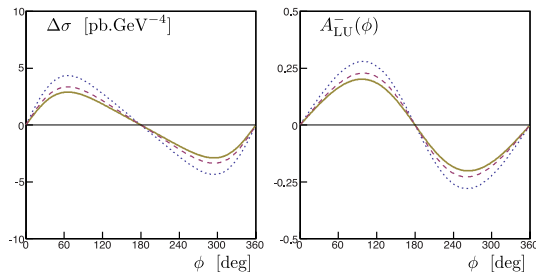


Figure 2: The difference of DVCS cross sections for opposite lepton helicities in pb/GeV^4 (left) and the corresponding asymmetry (right), as a function of ϕ for $E_e = 11\text{GeV}$, $\mu_F^2 = Q^2 = 4\text{GeV}^2$ and $t = -0.2\text{GeV}^2$. The GPD $H(x, \xi, t)$ is parametrized by the GK model. The contributions from other GPDs are not included.

of intermediate states in some channels which are kinematically forbidden in the DVCS case. This opens the way to new absorptive parts of the amplitude. To estimate Compton Form Factors (CFF), we use the NLO calculations of the coefficient functions which have been calculated in the DVCS case in the early days of GPD studies and more recently for the TCS case [4], the two results being simply related thanks to the analyticity (in Q^2) properties of the amplitude [6]:

$$TCS T(x, \eta) = \pm \left({}^{DVCS} T(x, \xi = \eta) + i\pi C_{coll}(x, \xi = \eta) \right)^* , \quad (5)$$

where $+$ ($-$) sign corresponds to vector (axial) case.

Using two GPD models based on Double Distributions (DDs), as discussed in detail in Ref. [5]: the Goloskokov-Kroll (GK) model [7] and a model based on the MSTW08 PDF parametrization [8], we get the results shown in Fig. 1 for the real and imaginary parts of the spacelike and timelike dominant CFF $\mathcal{H}(\xi, t)$ and $\mathcal{H}(\eta, t)$. Comparing dashed and solid lines in the upper panels, one sees that gluonic contributions are so important that they even change the sign of the real part of the CFF, and are dominant for almost all values of the skewness parameter. A milder conclusion arises from a similar comparison of the lower panels; the gluonic contribution to the imaginary part of the CFF remains sizeable for values of the skewness parameter up to 0.3.

2.2 Gluonic effects to DVCS observables

The effects of NLO contributions to some of the DVCS observables at moderate energies are exemplified in Fig. 2 and Fig. 3 which show specific observables to be measured at JLab and COMPASS. The difference between the dotted and solid lines demonstrates that NLO contributions are important, whereas the difference between the dashed and solid lines shows that gluon contributions should not be forgotten even at low energy when a precise data set is analyzed.

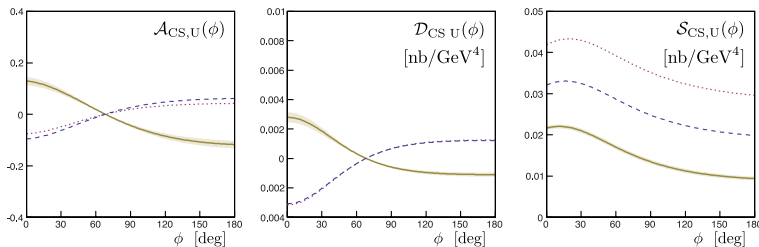


Figure 3: The DVCS observables for the COMPASS experiment, from left to right, mixed charge-spin asymmetry, mixed charge-spin difference and mixed charge-spin sum (in nb/GeV⁴). The kinematical point is chosen as $\xi = 0.05, Q^2 = 4 \text{ GeV}^2, t = -0.2 \text{ GeV}^2$. The GPD $H(x, \xi, t)$ is parametrized in the double distribution model based on the MSTW08 parametrization. The contributions from other GPDs are not included.

3 TCS in ultraperipheral collisions

Timelike Compton scattering in ultraperipheral collisions at hadron colliders opens a new way to measure generalized parton distributions, in particular for very small values of the skewness parameter.

We estimated [9] the different contributions to the lepton pair cross section for ultraperipheral collisions at the LHC. Since the cross sections decrease rapidly with Q^2 , we are interested in the kinematics of moderate Q^2 , say a few GeV², and large energy, thus very small values of η . Note however that for a given proton energy the photon flux is higher at smaller photon energy.

The Bethe-Heitler amplitude grows much when small θ angles are allowed. In the following we will use the limits $[\pi/4, 3\pi/4]$ where the Bethe-Heitler cross section is sufficiently big but does not dominate too much over the Compton process. The Bethe-Heitler cross section integrated over $\theta \in [\pi/4, 3\pi/4], \phi \in [0, 2\pi], Q^2 \in [4.5, 5.5] \text{ GeV}^2, |t| \in [0.05, 0.25] \text{ GeV}^2$, as a function of γp energy squared s is in the limit of large s constant and equals 28.4 pb.

Since the amplitudes for the Compton and Bethe-Heitler processes transform with opposite signs under reversal of the lepton charge, the interference term between TCS and BH is odd under exchange of the ℓ^+ and ℓ^- momenta. It is thus possible to project out the interference term through a clever use of the angular distribution of the lepton pair. The interference part of the cross-section for $\gamma p \rightarrow \ell^+ \ell^- p$ with unpolarized protons and photons has a characteristic (θ, ϕ) dependence given by (see details in [9])

$$\frac{d\sigma_{INT}}{dQ^2 dt d\cos\theta d\phi} = -\frac{\alpha_{em}^3}{4\pi s^2} \frac{1}{-t} \frac{M}{Q} \frac{1}{\tau\sqrt{1-\tau}} \cos\phi \frac{1+\cos^2\theta}{\sin\theta} \mathcal{Re}\mathcal{M},$$

with

$$\mathcal{M} = \frac{2\sqrt{t_0-t}}{M} \frac{1-\eta}{1+\eta} \left[F_1 \mathcal{H}_1 - \eta(F_1 + F_2) \tilde{\mathcal{H}}_1 - \frac{t}{4M^2} F_2 \mathcal{E}_1 \right], \quad (6)$$

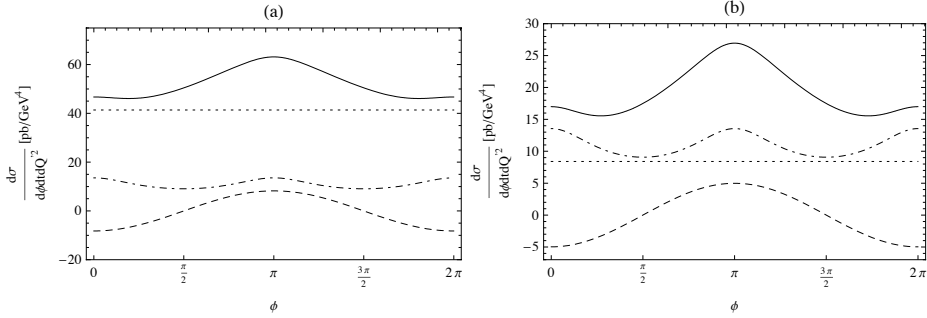


Figure 4: The lepton pair production differential cross sections (solid lines) for $t = -0.2 GeV^2$, $Q^2 = 5 GeV^2$ integrated over $\theta = [\pi/4, 3\pi/4]$, as a function of ϕ , for $s = 10^7 GeV^2$ (a), $s = 10^5 GeV^2$ (b) with $\mu_F^2 = 5 GeV^2$. We also display the Compton (dotted), Bethe-Heitler (dash-dotted) and Interference (dashed) contributions.

where $\tau = Q^2/s$, $-t_0 = 4\eta^2 M^2/(1-\eta^2)$ and $\mathcal{H}, \tilde{\mathcal{H}}, \mathcal{E}$ are Compton form factors. With the integration limits symmetric about $\theta = \pi/2$ the interference term changes sign under $\phi \rightarrow \pi + \phi$ due to charge conjugation, whereas the TCS and BH cross sections do not. One may thus extract the Compton amplitude

$$\int_0^{2\pi} d\phi \cos\phi \frac{d\sigma}{d\phi}.$$

In Fig. 4 we show the interference contribution to the cross section in comparison to the Bethe-Heitler and Compton processes, for various values of photon proton energy squared $s = 10^7 GeV^2, 10^5 GeV^2$. We observe that for larger energies the Compton process dominates, whereas for $s = 10^5 GeV^2$ all contributions are comparable.

4 Ultraperipheral collisions in a high-energy fixed-target experiment AFTER@LHC

The main idea of the multi-purpose project AFTER@LHC is to extract the halo of the LHC proton or ion beams by means of a bent-crystal and to use it as a beam in the fixed-target experiments [10]. The extracted beams will have a sufficiently high energy to produce on fixed target in ultraperipheral scattering a lepton pair with high invariant mass or heavy mesons. In these experiments a nucleus projectile or a nucleus target is treated as a high-energy photon source which allows study of photon-hadron collisions. Fig. 5 (and 6 respectively) shows preliminary estimates of the Bethe-Heitler, TCS, and Interference contributions to the cross section, as functions of the CMS rapidity y , after integration over $\theta \in (\pi/4, 3\pi/4)$, in the region where the interference contribution is best seen, for the collision of a proton beam with a Pb target (and of a Pb beam with a proton target respectively). The double distribution model of GPDs based on

MSTW08 parametrization is used.

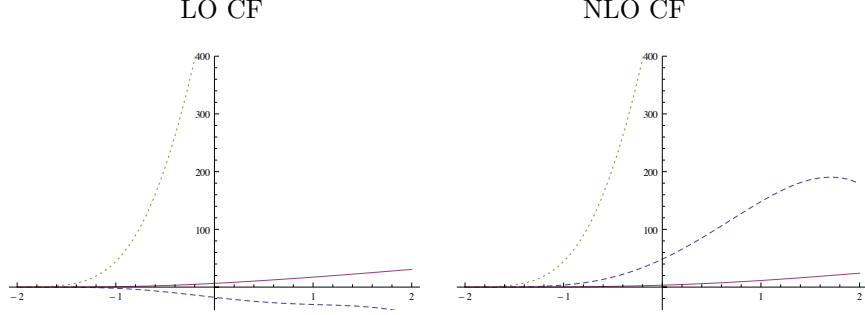


Figure 5: The Bethe-Heitler(dotted), TCS(solid) and Interference(dashed) contributions to $\frac{d\sigma}{dQ^2 dt dy d\phi}$ in pb/GeV^4 as a function of y (in CMS) for $Q^2 = 4GeV^2$, $t = -0.1GeV^2$, $\phi = 0$ for the proton beam and Pb target case.

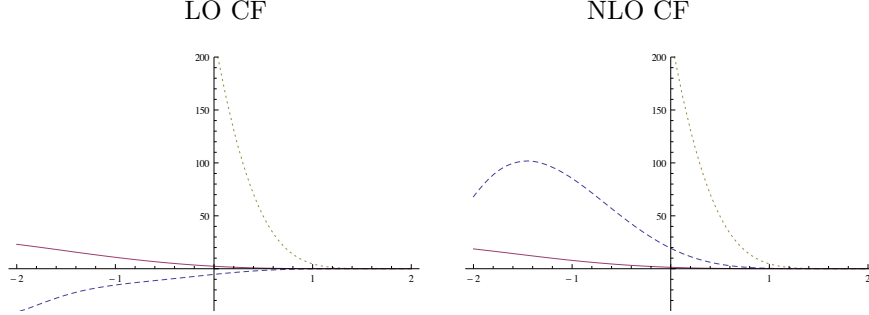


Figure 6: The Bethe-Heitler(dotted), TCS(solid) and Interference(dashed) contributions to $\frac{d\sigma}{dQ^2 dt dy d\phi}$ in pb/GeV^4 for BH(dotted), TCS(solid), Interference(dashed) as a function of y (in CMS) for $Q^2 = 4GeV^2$, $t = -0.1GeV^2$, $\phi = 0$, for the Pb beam and proton target case.

5 Summary and outlook

We did not discuss here the rich phenomenology of DVCS and TCS processes which electron-ion colliders [12] will allow to study. Neither did we comment on recent progresses in higher twist contributions [13] nor on the effect of resummation of higher order QCD corrections [14]. The physics of generalized parton distributions is definitely a domain of work in progress, both on the theory and on the experimental side.

Acknowledgments

This work is supported by the Polish Grant NCN No DEC- 2011/01/D/ST2/03915, the French-Polish collaboration agreement Polonium, the ANR project "Partons", the COPIN-IN2P3 Agreement and the Joint Research Activity "Study of Strongly Interacting Matter" (HadronPhysics3, Grant Agreement n.283286) under the 7th Framework Programm of the European Community.

References

- [1] D. Müller *et al.*, Fortsch. Phys. **42**, 101 (1994); A. V. Radyushkin, Phys. Lett. B **380**, 417 (1996); X. D. Ji and J. Osborne, Phys. Rev. D **58**, 094018 (1998); J. Collins and A. Freund, Phys. Rev. **D59**, 074009 (1999).
- [2] E. R. Berger, M. Diehl and B. Pire, Eur. Phys. J. C **23** (2002) 675.
- [3] K. Goetze, M. V. Polyakov and M. Vanderhaeghen, Prog. Part. Nucl. Phys. **47**, 401 (2001); M. Diehl, Phys. Rept. **388**, 41 (2003); A. V. Belitsky and A. V. Radyushkin, Phys. Rept. **418**, 1 (2005).
- [4] B. Pire, L. Szymanowski and J. Wagner, Phys. Rev. D **83** (2011) 034009; Few Body Syst. **53** (2012) 125.
- [5] H. Moutarde, B. Pire, F. Sabatie, L. Szymanowski and J. Wagner, Phys. Rev. D **87** (2013) 054029.
- [6] D. Mueller, B. Pire, L. Szymanowski and J. Wagner, Phys. Rev. D **86** (2012) 031502.
- [7] S. V. Goloskokov and P. Kroll, Eur. Phys. J. C **53**, 367 (2008).
- [8] A. D. Martin, W. J. Stirling, R. S. Thorne and G. Watt, Eur. Phys. J. C **63**, 189 (2009).
- [9] B. Pire, L. Szymanowski and J. Wagner, Phys. Rev. D **79** (2009) 014010, Acta Phys. Polon. Supp. **2** (2009) 373 and Nucl. Phys. Proc. Suppl. **179-180** (2008) 232.
- [10] S. J. Brodsky, F. Fleuret, C. Hadjidakis, J.P. Lansberg, Phys. Rep. **522** (2013) 239; J.P. Lansberg et al, arXiv:1308.5806.
- [11] J.P. Lansberg, L. Szymanowski and J. Wagner, in preparation.
- [12] D. Boer *et al.*, arXiv:1108.1713 [nucl-th]; J. L. Abelleira Fernandez *et al.* [LHeC Study Group Collaboration], J. Phys. G **39**, 075001 (2012).
- [13] V. M. Braun, A. N. Manashov and B. Pirnay, Phys. Rev. Lett. **109**, 242001 (2012); B. Pire, L. Szymanowski and S. Wallon, arXiv:1309.0083 [hep-ph].
- [14] T. Altinoluk, B. Pire, L. Szymanowski and S. Wallon, JHEP **1210** (2012) 049 and these proceedings.